Hindawi
Journal of Nanomaterials
Volume 2019, Article ID 8364740, 7 pages
https://doi.org/10.1155/2019/8364740

Research Article

Fabrication of MoS_2 Nanoflakes Supported on Carbon Nanotubes for High Performance Anode in Lithium-Ion Batteries (LIBs)

T. Minh Nguyet Nguyen,[1] Vinh-Dat Vuong,[1,2] Mai Thanh Phong,[3] and Thang Van Le[1,2]

[1]*VNU-HCM Key Laboratory for Material Technologies, HCMUT, VNU-HCM, Ho Chi Minh City 740128, Vietnam*
[2]*Department of Energy Materials, Faculty of Materials Technology, HCMUT, VNU-HCM, Ho Chi Minh City 740128, Vietnam*
[3]*Ho Chi Minh City University of Technology, VNU-HCM, Ho Chi Minh City 740128, Vietnam*

Correspondence should be addressed to Thang Van Le; vanthang@hcmut.edu.vn

Received 23 April 2019; Revised 16 August 2019; Accepted 2 December 2019; Published 28 December 2019

Academic Editor: Yu-Lun Chueh

Copyright © 2019 T. Minh Nguyet Nguyen et al. This is an open access article distributed under the Creative Commons Attribution License, which permits unrestricted use, distribution, and reproduction in any medium, provided the original work is properly cited.

Molybdenum disulfide (MoS_2), an inorganic-layered material similar to structure of graphite, was randomly dispersed onto the surface of functionalized multiwalled carbon nanotubes to synthesized nanocomposite MoS_2/CNT. The as-obtained product was characterized via SEM, TEM, TGA, X-ray diffraction, and Raman spectroscopies. It was confirmed from XRD that MoS_2 layers with interlayer spacing of 0.614 nm were successfully produced. TEM images and Raman spectra indicated a random distribution of 20 nm sized nanoflake MoS_2 on the surface of MWNTs. The electrochemical performance of materials are expected to pave the way for the utilized anode material for lithium-ion batteries.

1. Introduction

For many years, energy storage is a major concern for all businesses and individuals. Many methods are developed to capture renewable energy sources such as solar cells, wind turbines, and tidal power. The conversion of these energy sources into direct electricity does not meet the demand for production and consumption. Storing energy obtained in the form of electricity, as rechargeable batteries, is an important solution. The emergence of rechargeable batteries in general and lithium-ion batteries (LIBs) in particular has become an effective alternative to battery research.

In landscape of LIBs, transition metal dichalcogenide (TMD), especially molybdenum disulfide (MoS_2), has currently attracted considerable attention due to its important role in many applications. In literature of knowledge, MoS_2 present its potential in areas, such as catalysts for the hydrogen evolution reaction (HER) [1], photoelectrode for energy conversion [2], lithium or sodium batteries [3], chemical sensing [3, 4], fillers in polymer composites [5, 6], photocatalysts [7–9], and solid lubricants for metallic and ceramic surfaces [10]. In recent years, MoS_2 has emerged as a promising anode material in lithium-ion batteries (LIBs) due to its typical-layered transition metal sulfide composing of three stacked atom layers (S-Mo-S) (Figure 1) [10]. Such MoS_2 nanostructures have a large specific surface area as well as abundant voids and defects that may provide more and shorter Li-ion diffusion during lithiation/delithiation processes [11]. In addition, the weak van der Waals interaction between MoS_2 layers allows the diffusion of Li^+ ions without significant volumetric change during charge/discharge processes.

However, the poor electrical conductivity, low cycling stability, and high agglomerate risk remain the major drawbacks of bulk MoS_2. To overcome these problems, numerous studies of growth of MoS_2 on different conductive substrate or supports, such carbon paper [12–15], graphite [12, 13], 1D carbon nanotubes (CNTs) [10, 11, 14, 16–19], 3D nanocarbon [20], carbon nanofiber [21], or graphene [10, 14, 22, 23], were

conducted to improve their electrochemical performance and stability. Well reversible specific capacity as high as 1,290 $mAh \cdot g^{-1}$ were reported for nanostructured MoS_2-graphene anodes [10, 14]. Nanocomposite of MoS_2 and carbon nanotubes also remains attractive in terms of capacity. For example, MoS_2 nanosheet decorated on multiwalled carbon nanotubes (MWNTs) and single-walled carbon nanotubes (SWNTs) reported as larger than 1,000 and 1,400 $mAh \cdot g^{-1}$, respectively. Constructing a composite material with reduced MoS_2 agglomerate on an interconnected conducting network of CNTs is crucial for high-rate capability and long-term cyclability of lithium-ion battery.

To date, the synthesis of MoS_2 nanomaterials has mainly been based on reactions in liquid media, i.e., hydrothermal [24], solvothermal [22], or even sonochemical synthesis [25]. Significant number of publications demonstrated that mass loadings of nanocomposite of MoS_2 and carbon-based materials can be created by hydrothermal synthesis. Also, solvothermal-synthesized nanoflake MoS_2 was reported with 700–800 $mAh \cdot g^{-1}$ specific capacity. Although nanosized MoS_2 with different morphologies has successfully been prepared, the synthesized conditions are generally carried out under harsh conditions with high temperatures and pressures. Herein, a facile method was reported using gentle synthesis procedure to prepare MoS_2 nanoflakes with the support of MWNTs. Using our experimental procedure, MoS_2 nanoflakes with thickness of ~ 20 nm were readily obtained and randomly dispersed onto the surface of carbon nanotubes. Moreover, the MoS_2 interlayer spacing was around 0.62 nm, which makes them attractive for applications in lithium batteries.

2. Materials and Methods

The raw MWNTs were produced by the thermal chemical vapor deposition (T-CVD) method and purified by the wet chemical method. The details for MWNT synthesis and purification were given elsewhere [26–28]. For a better wetting of the surface, MWNTs were treated by refluxing in a mixture of $C_6H_7NSO_3$ and $NaNO_2$ [29].

All the chemicals used in this work were of reagent grade. Ammonium heptamolybdate tetrahydrate $(NH_4)_6Mo_7O_{24} \cdot 4H_2O$, sodium sulfide nonahydrate $Na_2S \cdot 9H_2O$, and ethylene glycol were purchased from Merck.

86.5 mg of $(NH_4)_6Mo_7O_{24} \cdot 4H_2O$ was immersed into 50 mL of deionized water (DI) and sonicated until being completely dissolved to achieve a homogeneous solution. Then, 960 mg of $Na_2S \cdot 9H_2O$ and 50 mg of MWNTs were added into the suspension and dispersed via sonication for 5 min to obtain a precursor solution. 50 mL of ethylene glycol was mixed with the precursor solution, and the reaction was carried out at 80°C for 30 min under stirring with gradual dropping of 2 mL of 1 M HCl solution. After that, the precipitates were collected, washed with DI water, and dried at 80°C in an oven.

The morphology and structure of the prepared samples were analyzed by TEM (JEOL-JEM-1400), SEM (JEOL-JSM-7401F), XRD (D8 ADVANCE), Raman (Labram 300), TGA (Netzsch TG 209 F3). The electrochemical measurements were performed by PARSTAT 2273 instrument using a Swagelok cell, where counter electrode was a lithium foil, reference electrode was Li/Li^+, and working electrode was prepared by the following steps:

(i) 15 mg of composite material binder free was compressed on a 10 mm in diameter discs of copper foil

(ii) 3 layers of Nafion membrane were soaked with few drops of 1 M $LiPF_6$ in EC : DMC (1 : 1 *v*/*v*) solution, then sandwiched between the composite working electrode and counter electrode

(iii) the entire assembly was secured in a cylinder of Swagelok cell

All the electrode preparing process and cyclic voltammetry were accomplished in argon full filled glovebox. The cyclic voltammograms were obtained from 0 to 3.5 V (versus Li/Li^+) of voltage range at 1 mV/s of scanning rate.

3. Results and Discussion

Figure 2 shows XRD patterns of MoS_2 prepared with and without CNTs. The diffraction peaks of MWNTs appeared at 2θ of about 26° and 53° corresponding to (002) and (004) planes (according to JCPDS 25-0284), respectively (Figures 2(a) and 2(c)). Four other distinct peaks at 2θ of 14.41°, 32.76°, 39.60°, and 58.31° corresponding to (002), (100), (103) and (110) planes of MoS_2 (according to JCPDS 37-1492), respectively, were observed (Figures 2(b) and 2(c)). The d-spacing for the (002) plane of MoS_2 layers was calculated to be 0.617 nm according to its diffraction peak at $2\theta = 14.34°$ using Bragg's equation, which is consistent with that of hexagonal MoS_2 (2H-MoS_2) [27]. It should be noted that the relative diffraction peak intensities of the MoS_2/CNT sample are enhanced in comparison with those of MoS_2 obtained in the absence of CNTs. The enhanced diffraction peaks indicate that the MoS_2 layers growing on CNTs have higher crystallinity than that obtained in the absence of CNTs. This also demonstrates that CNTs can support the formation of MoS_2 and improve its crystallinity. In the case of MoS_2/CNTs, the (002) plane diffraction peak has a small shift to a lower angle of 14.34° from the standard angle of 14.41°, indicating that the interlayer distance of the MoS_2 nanoflakes is slightly increased which will potentially provide a sufficiently larger space for lithium-ion intercalation. It has been reported that with 1 mol of lithium intercalation, the c parameter of MoS_2 undergoes an increment of 0.03 Å. The expanded interlayer d-spacing would relieve the strain caused by electrochemical lithiation/delithiation during cycling and provide more space for Li-ion intercalation with reduced diffusion barriers [11, 30, 31].

To verify the morphology of the as-prepared product, scanning electron microscopy (SEM) and transmission electron microscopy (TEM) were conducted. The surface morphology of MoS_2 and carbon nanotubes could be clearly observed in Figures 3(a) and 3(b). Figure 3(a) illustrates that MoS_2 obtained in the absence of CNTs composes of nanoflake coalescence into large particles. The average crystallite

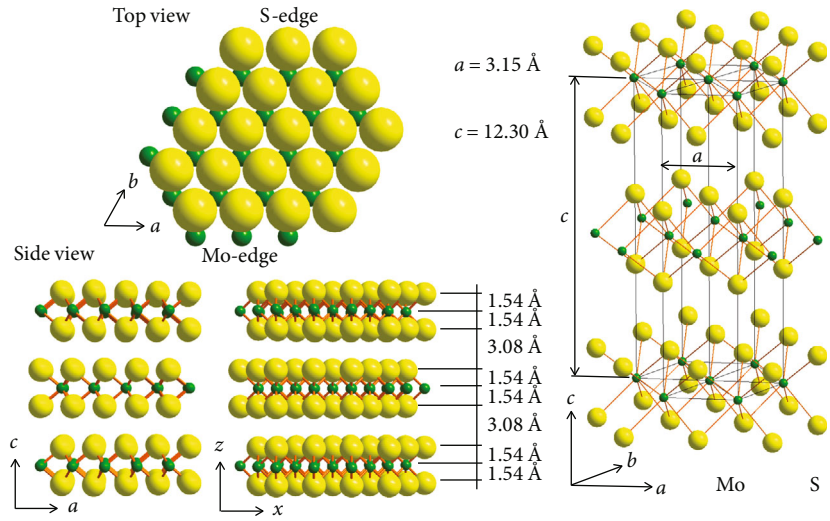

Figure 1: Structure of molybdenum disulfide.

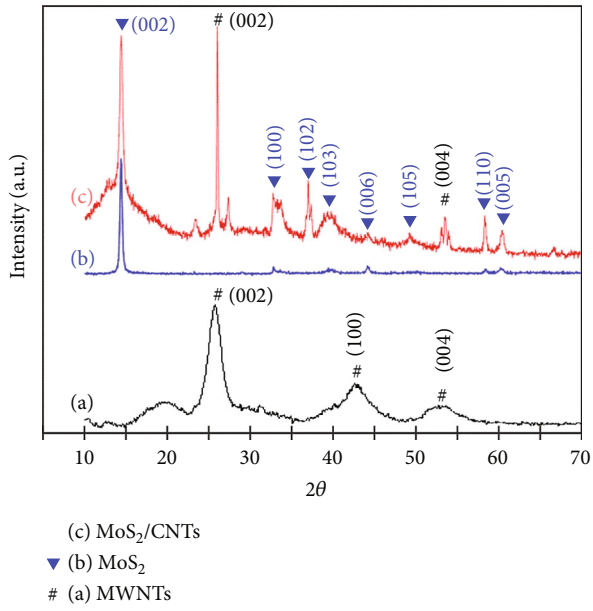

Figure 2: XRD patterns of (a) MoS_2/CNTs and (b) MoS_2 prepared in the absence of CNTs.

size of the nanoflakes is around 20 nm in the thickness direction. In the presence of CNTs, a similar morphology of MoS_2 is observed under TEM. However, the MoS_2 nanoflakes appeared to be randomly distributed on the surface of CNTs in contrast to the agglomeration of MoS_2 nanoflakes synthesized without CNTs (Figures 3(c) and 3(d)).

Raman spectroscopy was also employed to further characterize the MoS_2/CNT hybrid structure. Raman experiments were carried out with 632.8 nm excitation. Figures 4(a) and 4(b) compare the Raman spectra taken from the as-obtained MoS_2/CNTs and bare CNTs. The Raman peaks at around 1573 cm^{-1} and 1325 cm^{-1} belong to MWNTs, while the G′ band of MWNTs is located at 2,650 cm^{-1}, consistent with previous reports [28]. The appearance of two other peaks at 377 and 405 cm^{-1} corresponds to the out-of-plane (A_{1g}) and in-plane ($E_{2g}{}^1$) vibrational modes of hexagonal MoS_2, respectively. A more detailed view of the vibrational modes is presented in Figure 4(c). Two MoS_2 layers and corresponding vibrations are displayed. The ratio of these two peaks is usually employed to evaluate the thickness and orientation of MoS_2 [32–36]. The MoS_2 thin sheets with the basal plane exposed to laser beam (composed of less than 10 layers) are often reported to have this value being about 1, while this value of the bulk ones is about 1.5. In contrary, a value above 3 was reported for the nanosheet (NS) with the edge side exposed to laser beam [32–37]. The peak intensity ratio was observed to be higher than 3 (approximately 4) in this study, suggesting that the MoS_2 NS growth direction is perpendicular to the CNT surface.

New peaks at around 450 cm^{-1} and 630 cm^{-1} (Figure 4(b)) might be caused by the MoS_2 being partially oxidized if the laser power was too large and focused on the sample in the measurement. It was also found that the signals related to the CNTs mostly overlap with those of the MoS_2 sheets, and their intensity becomes significantly weaker, which suggests a good grafting of MoS_2 around the surface of CNTs.

The thermogravimetric analysis curves (Figure 5) were used to calculate the loading percentage of MoS_2 in the nanocomposite. Similar TGA curves for bare MoS_2 and MoS_2/CNTs showed the first mass loss from 100°C to about 200°C related to evaporation of absorbed moisture on the surface of materials. Larger specific area of MoS_2/CNTs allowed it containing more moisture that make evaporation of the sample occur at over 300°C. Afterward, the consecutive reaction is oxidation of MoS_2 to MoO_3 in air from 300°C. At over 400°C to 850°C, oxidation of CNTs occurred parallel to oxidation of MoS_2 in nanocomposite sample that makes its weight lose faster than bare MoS_2. The calculated results from TGA curves, MoS_2, and MWNTs in the nanocomposite have approximate loading percentage of 76 wt% and 24 wt%, respectively.

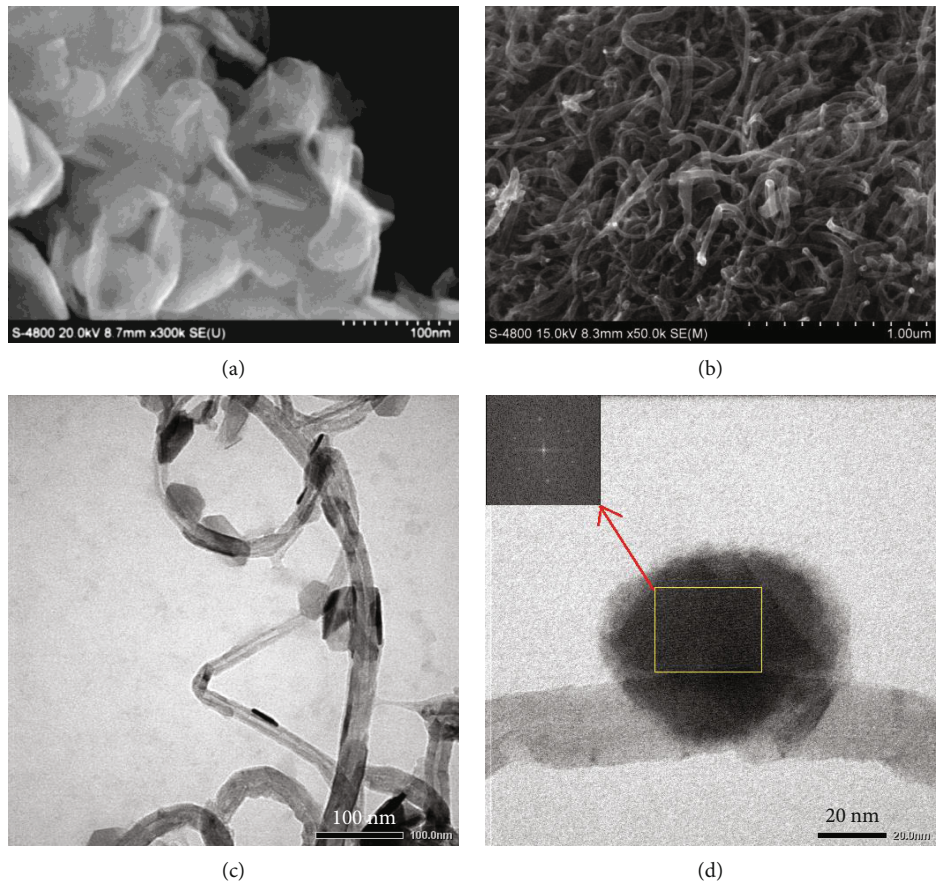

Figure 3: (a) SEM image of MoS_2 prepared in the absence of CNTs; (b) SEM image of prepared MoS_2/CNTs; (c, d) TEM images of MoS_2/CNTs. Inset in (d) shows the FFT patterns taken from the marked area.

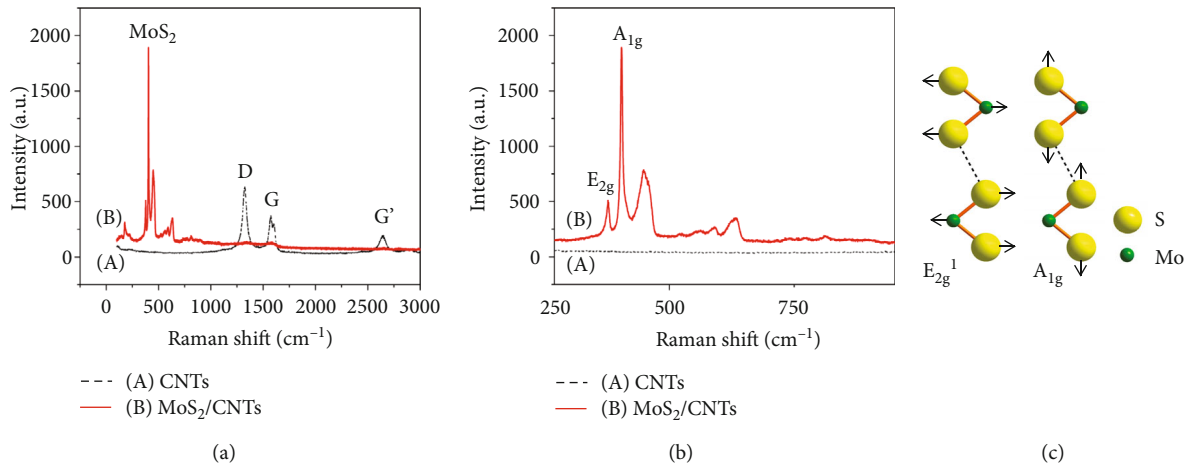

Figure 4: (a) Raman spectra of (A) MoS_2/CNTs and (B) bare CNTs; (b) comparison of the magnified Raman signals of MoS_2 in prepared MoS_2/CNTs and bare CNTs; (c) symmetric displacement of Mo and S atoms in A_{1g} and $E_{2g}{}^1$ vibrational modes.

Figure 6 showed voltammograms for prepared MoS_2/CNT anode materials. In knowledge of literature, lithiation of MoS_2 occurred within the voltage window of 3–0 V (vs. Li/Li^+). The first intercalation step of Li^+ into MoS_2 is shown as reaction (1) [17]. Reaction (1) is attributed by the peak at about 3.0 to 1.1 V. In the first scan, a reduction peak at approximately 1.1 to 1.2 V described the transformation of trigonal prismatic 2H-MoS_2 to octahedral 1T-Li_x-MoS_2 [17, 18]. The second peak at 0.6 to 0.7 V attributed to lithiation into MWNTs and the formation of Li_2S to release

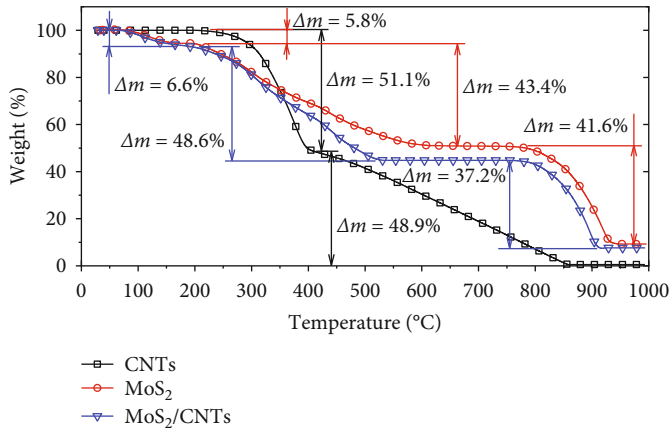

Figure 5: TGA curves for bare MWNTs, MoS_2, and prepared MoS_2/CNTs (heating in air with 10 K/min of rate, from room temperature to 980°C).

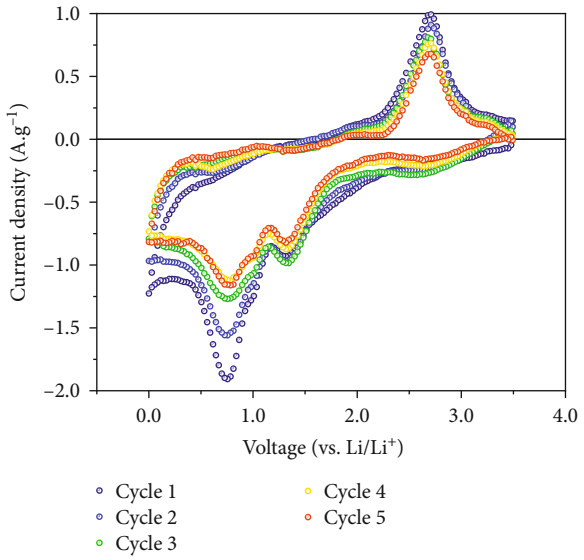

Figure 6: The cyclic voltammograms for MoS_2/CNTs as anode materials.

Mo which is shown as reaction (2) [17]. Lithiation peak of MoS_2/CNTs presented larger peak area than that of MoS_2 that mainly resulted higher capacity of MoS_2/CNTs.

$$MoS_2 + x\,Li^+ + x\,e^- \longrightarrow Li_xMoS_2 \quad (1)$$

$$Li_xMoS_2 + (4-x)\,Li^+ + (4-x)\,e^- \longrightarrow Mo + 2\,Li_2S \quad (2)$$

In charging scan, Figure 6 showed a shallow peak at 1.7–1.8 V and a large peak at 2.6–2.7 V, approximately. The first shallow peak attributed delithiation of enduring Li_xMoS_2 which was not conversed by reaction (2). The officious delithiation step is the conversion of Li_2S to S_8^{2-}, which is attributed by the large peak at 2.6–2.7 V. The reversible conversion of MoS_2/CNTs demonstrates the absence or the exiguous formation of rigid Li_2S, which is constantly attributed by disappeared peak at approximately 0.4 V.

4. Conclusions

In summary, nanoflake MoS_2 were grafted directly on the surface of carbon nanotubes. These MoS_2/CNT nanocomposites were conveniently synthesized by the wet-chemical process, in which grafted MoS_2 nanoflakes are high crystalline and likely to be grown parallel to the MWNT surface. The MoS_2 nanoflakes had about 20 nm size with the interlayer spacing of 0.614 nm, which makes their electrochemical performance suitable for applications in lithium batteries. The nanocomposite contained 24 wt% of CNTs to rise the rate of lithiation.

Data Availability

The SEM, TEM, XRD, and Raman spectroscopy used to support the findings of this study have not been made available because they were provided only as image data type by analysis centres.

Conflicts of Interest

The authors declare that there is no conflict of interest regarding the publication of this paper.

Acknowledgments

This research is funded by the Viet Nam National University Ho Chi Minh City (VNU-HCM) under grant number B2017-20-07/HĐ-KHCN.

Supplementary Materials

S1: materials. Synthesis and purification of multiwalled carbon nanotubes (MWNTs). Surface treatment of MWNTs. S2: cyclic voltammograms of MoS_2/CNTs. *(Supplementary Materials)*

References

[1] Y. Yan, B. Xia, Z. Xu, and X. Wang, "Recent development of molybdenum sulfides as advanced electrocatalysts for

hydrogen evolution reaction," *ACS Catalysis*, vol. 4, no. 6, pp. 1693–1705, 2014.

[2] S. V. Prabhakar Vattikuti, "Recent trends and developments in transition metal dichalcogenide photoelectrodes for solar-to-hydrogen conversion," *Journal of Electrochemical Energy Conversion and Storage*, vol. 15, no. 4, article 041003, 2018.

[3] H. Li, J. Wu, Z. Yin, and H. Zhang, "Preparation and applications of mechanically exfoliated single-layer and multilayer MoS_2 and WSe_2 nanosheets," *Accounts of Chemical Research*, vol. 47, no. 4, pp. 1067–1075, 2014.

[4] S. V. Prabhakar Vattikuti and C. Byon, "Synthesis and structural characterization of Al_2O_3-coated MoS_2 spheres for photocatalysis applications," *Journal of Nanomaterials*, vol. 2015, Article ID 978409, 9 pages, 2015.

[5] Z. Matusinovic, R. Shukla, E. Manias, C. G. Hogshead, and C. A. Wilkie, "Polystyrene/molybdenum disulfide and poly(methyl methacrylate)/molybdenum disulfide nanocomposites with enhanced thermal stability," *Polymer Degradation and Stability*, vol. 97, no. 12, pp. 2481–2486, 2012.

[6] M. B. Khan, R. Jan, A. Habib, and A. N. Khan, "Evaluating mechanical properties of few layers MoS_2 nanosheets-polymer composites," *Advances in Materials Science and Engineering*, vol. 2017, Article ID 3176808, 6 pages, 2017.

[7] S. V. P. Vattikuti, P. C. Nagajyothi, and J. Shim, "Use of lactic acid modified MoS2nanopetals to improve photocatalytic degradation of organic pollutants," *Materials Research Express*, vol. 5, no. 9, article 095016, 2018.

[8] S. V. P. Vattikuti and C. Byon, "Bi_2S_3 nanorods embedded with MoS_2 nanosheets composite for photodegradation of phenol red under visible light irradiation," *Superlattices and Microstructures*, vol. 100, pp. 514–525, 2016.

[9] S. V. P. Vattikuti and C. Byon, "Hydrothermally synthesized ternary heterostructured $MoS_2/Al_2O_3/g\text{-}C_3N_4$ photocatalyst," *Materials Research Bulletin*, vol. 96, pp. 233–245, 2017.

[10] T. Stephenson, Z. Li, B. Olsen, and D. Mitlin, "Lithium ion battery applications of molybdenum disulfide (MoS_2) nanocomposites," *Energy & Environmental Science*, vol. 7, no. 1, pp. 209–231, 2014.

[11] C. Zhao, J. Kong, X. Yao et al., "Thin MoS_2 nanoflakes encapsulated in carbon nanofibers as high-performance anodes for lithium-ion batteries," *ACS Applied Materials & Interfaces*, vol. 6, no. 9, pp. 6392–6398, 2014.

[12] X. Xie, T. Makaryan, M. Zhao, K. L. van Aken, Y. Gogotsi, and G. Wang, "MoS2Nanosheets vertically aligned on carbon paper: a freestanding electrode for highly reversible sodium-ion batteries," *Advanced Energy Materials*, vol. 6, no. 5, article 1502161, 2016.

[13] J. Li, Y. Jiang, F. Qin, J. Fang, K. Zhang, and Y. Lai, "Magnetron-sputtering MoS_2 on carbon paper and its application as interlayer for high-performance lithium sulfur batteries," *Journal of Electroanalytical Chemistry*, vol. 823, pp. 537–544, 2018.

[14] L. Zhang, W. Fana, and T. Liu, "A flexible free-standing defect-rich MoS_2/graphene/carbon nanotube hybrid paper as a binder-free anode for high-performance lithium ion batteries," *RSC Advances*, vol. 5, no. 54, pp. 43130–43140, 2015.

[15] H. Yang, M. Wang, X. Liu, Y. Jiang, and Y. Yu, "MoS_2 embedded in 3D interconnected carbon nanofiber film as a free-standing anode for sodium-ion batteries," *Nano Research*, vol. 11, no. 7, pp. 3844–3853, 2018.

[16] X.-M. Liu, Z. Huang, S. Oh et al., "Carbon nanotube (CNT)-based composites as electrode material for rechargeable Li-ion batteries: a review," *Composites Science and Technology*, vol. 72, no. 2, pp. 121–144, 2012.

[17] Y. Shi, Y. Wang, J. I. Wong, A. Y. Tan, C. L. Hsu, and L. J. Li, "Self-assembly of hierarchical MoS_x/CNT nanocomposites ($2<x<3$): towards high performance anode materials for lithium ion batteries," *Scientific Reports*, vol. 3, no. 1, article 2169, 2013.

[18] K. Bindumadhavan, S. K. Srivastava, and S. Mahanty, "MoS_2-MWCNT hybrids as a superior anode in lithium-ion batteries," *Chemical Communications*, vol. 49, no. 18, pp. 1823–1825, 2013.

[19] C. Lu, W. W. Liu, H. Li, and B. K. Tay, "A binder-free CNT network-MoS_2 composite as a high performance anode material in lithium ion batteries," *Chemical Communications*, vol. 50, no. 25, pp. 3338–3340, 2014.

[20] C. Cui, X. Li, Z. Hu, J. Xu, H. Liu, and J. Ma, "Growth of MoS_2@C nanobowls as a lithium-ion battery anode material," *RSC Advances*, vol. 5, no. 112, pp. 92506–92514, 2015.

[21] R. Zhou, J.-G. Wang, H. Liu et al., "Coaxial MoS_2@carbon hybrid fibers: a low-cost anode material for high-performance Li-ion batteries," *Materials*, vol. 10, no. 2, p. 174, 2017.

[22] H. Hwang, H. Kim, and J. Cho, "MoS_2 nanoplates consisting of disordered graphene-like layers for high rate lithium battery anode materials," *Nano Letters*, vol. 11, no. 11, pp. 4826–4830, 2011.

[23] X. Cao, Y. Shi, W. Shi et al., "Preparation of MoS_2-coated three-dimensional graphene networks for high-performance anode material in lithium-ion batteries," *Small*, vol. 9, no. 20, pp. 3433–3438, 2013.

[24] R. Wei, H. Yang, K. Du et al., "A facile method to prepare MoS_2 with nanoflower-like morphology," *Materials Chemistry and Physics*, vol. 108, no. 2-3, pp. 188–191, 2008.

[25] I. Uzcanga, I. Bezverkhyy, P. Afanasiev, C. Scott, and M. Vrinat, "Sonochemical preparation of $_{MoS2in}$ Aqueous Solution: Replication of the cavitation bubbles in an inorganic material morphology," *Chemistry of Materials*, vol. 17, no. 14, pp. 3575–3577, 2005.

[26] T. M. N. Nguyen, D. V. Cao, T. A. Luu, and T. V. Le, "Synthesis of multiwall carbon nanotubes (MWCNTS) from acetylene decomposition over iron/nickel catalyst supported on alumina," *Journal of Science and Technology*, vol. 51, no. 5C, pp. 592–599, 2013.

[27] T. V. Le, H. T. Nguyen, A. T. Luu, M. V. Tran, and P. L. M. Le, "$LiMn_2O_4$/CNTs and $LiNi_{0.5}Mn_{1.5}O_4$/CNTs nanocomposites as high-performance cathode materials for lithium-ion batteries," *Acta Metallurgica Sinica (English Letters)*, vol. 28, no. 1, pp. 122–128, 2014.

[28] T. M. N. Nguyen, T. V. Le, V. D. Nguyen, T. H. Nguyen, T. A. Luu, and D. V. Cao, "A facile and effective purification method for multi-walled carbon nanotubes (MWNTS)," *Journal of Science and Technology*, vol. 49, no. 6C, pp. 279–286, 2011.

[29] V. D. Nguyen, H. T. Vu, T. M. N. Nguyen, H. T. Nguyen, and T. V. Le, "Diazonium functionalization of multiwall carbon nanotubes (MWCNTS) for carrying MoS_2 nanoparticles," *Journal of Science and Technology*, vol. 51, no. 5C, pp. 215–222, 2013.

[30] M. Wang, G. Li, H. Xu, Y. Qian, and J. Yang, "Enhanced lithium storage performances of hierarchical hollow MoS2-Nanoparticles assembled from nanosheets," *ACS Applied Materials & Interfaces*, vol. 5, no. 3, pp. 1003–1008, 2013.

[31] G. Du, Z. Gou, S. Wang, R. Zeng, Z. Chen, and H. Liu, "Superior stability and high capacity of restacked molybdenum disulfide as anode material for lithium ion batteries," *Chemical Communications*, vol. 46, no. 7, pp. 1106–1108, 2010.

[32] D. Kong, H. Wang, J. J. Cha et al., "Synthesis of MoS_2 and $MoSe_2$ films with vertically aligned layers," *Nano Letters*, vol. 13, no. 3, pp. 1341–1347, 2013.

[33] A. Splendiani, L. Sun, Y. Zhang, T. Li, J. Kim, and C. Y. Chim, "Emerging photoluminescence in monolayer MoS_2," *Nano Letters*, vol. 10, no. 4, pp. 1271–1275, 2010.

[34] G. Eda, H. Yamaguchi, D. Voiry, T. Fujita, M. Chen, and M. Chhowalla, "Photoluminescence from chemically exfoliated MoS_2," *Nano Letters*, vol. 11, no. 12, pp. 5111–5116, 2011.

[35] D. J. Late, B. Liu, R. H. S. S. Matte, V. P. Dravid, and C. N. R. Rao, "Hysteresis in single-layer MoS2Field effect transistors," *ACS Nano*, vol. 6, no. 6, pp. 5635–5641, 2012.

[36] S. Balendhran, J. Z. Ou, M. Bhaskaran et al., "Atomically thin layers of MoS_2 via a two step thermal evaporation-exfoliation method," *Nanoscale*, vol. 4, no. 2, pp. 461–466, 2012.

[37] N. H. H. Phuc, T. Okuno, and N. Hakiri, "Synthesis of high-edge exposure MoS_2 nano flakes," *Journal of Nanoparticle Research*, vol. 16, no. 1, article 2199, 2013.


The Scientific
World Journal
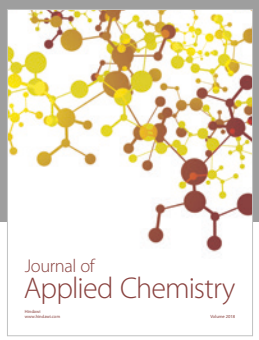
Journal of
Applied Chemistry
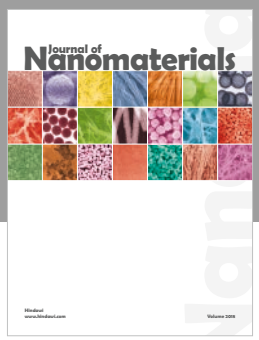
Journal of
Nanomaterials

Scientifica

International Journal of
Polymer Science
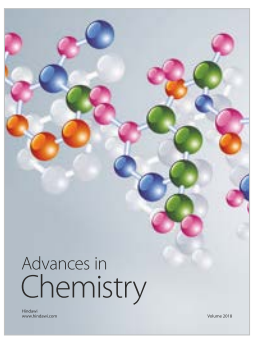
Advances in
Chemistry

Hindawi
Submit your manuscripts at
www.hindawi.com
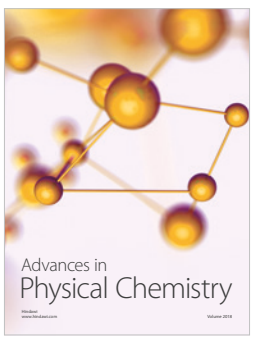
Advances in
Physical Chemistry

International Journal of
Analytical Chemistry
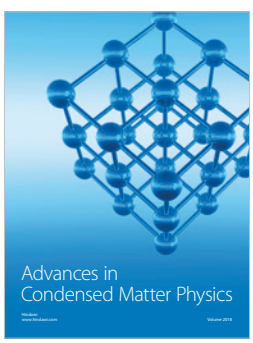
Advances in
Condensed Matter Physics
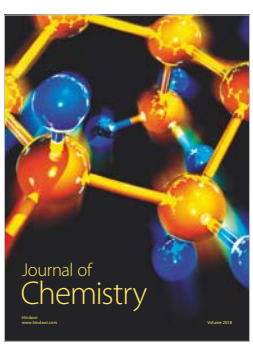
Journal of
Chemistry

International Journal of
Biomaterials
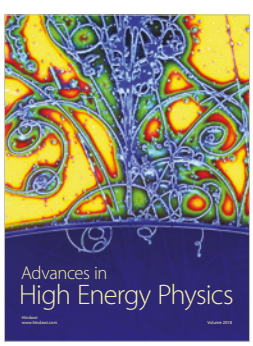
Advances in
High Energy Physics

Journal of
Engineering

Journal of
Nanotechnology

International Journal of
Corrosion

Journal of
Materials

BioMed
Research International
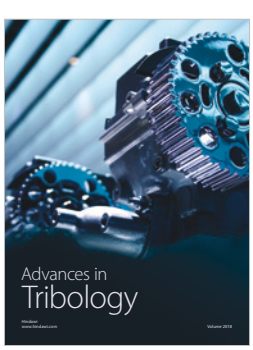
Advances in
Tribology
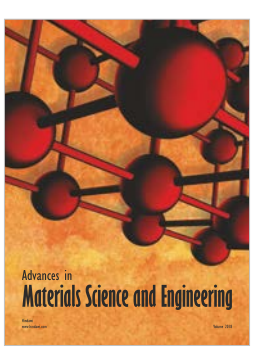
Advances in
Materials Science and Engineering